Shear Characterization of Unidirectional Composites with the Off-Axis Tension Test

by M.-J. Pindera and C.T. Herakovich

ABSTRACT—The influence of end constraints on accurate determination of the intralaminar shear modulus G_{12} from an off-axis tension test is examined both analytically and experimentally. The Pagano-Halpin model is employed to illustrate that, when the effect of end constraints is properly considered, the exact expression for G_{12} is obtained. When the effect of end constraints is neglected, expressions for the apparent shear modulus G_{12}^{*} and apparent Young's modulus E_{xx}^{*} are obtained. Numerical comparison for various off-axis configurations and aspect ratios is carried out using typical material properties for graphite/polyimide unidirectional composites. It is demonstrated that the end-constraint effect influences accurate determination of G_{12} more adversely than it affects the laminate Young's modulus E_{xx} in the low off-axis range. Experimental results obtained from off-axis tests on unidirectional Gr/Pi specimens confirm the above. Based on the presented analytical and experimental evidence, the 45-deg off-axis coupon is proposed for the determination of the intralaminar shear modulus G_{12}.

Introduction

The tensile test on unidirectional off-axis fiber composites is a fundamental test which has been successfully employed for a number of years by composites researchers to characterize the response of these advanced materials. Not only has the test been used to obtain such in-plane lamina properties as E_{11}, E_{22}, ν_{12} and the related strengths, but also to verify the material-symmetry assumptions of the particular system. The off-axis configuration has also been employed by numerous researchers in determining the in-plane or intralaminar shear modulus G_{12}. It is an attractive alternative to performing direct torsion tests on thin composite tubes which are more difficult and expensive to fabricate. The simplicity of employing the off-axis geometry to characterize the shear response of a unidirectional lamina has resulted in a proposal to employ the 10-deg off-axis configuration for such characterization.[1] This particular configuration has been chosen because it yields a high value of the shear strain γ_{12} at failure with the corresponding shear stress τ_{12} being the major stress contribution to fracture as determined from a combined-stress failure criterion.[2]

On the other hand, it has been known for some time that the off-axis configuration can introduce errors in the measured values of the laminate elastic material parameters due to the end-constraint effect.[3] The extent of the introduced error depends not only on the off-axis angle, specimen geometry, end contraint and degree of material anisotropy, but is also different for different material parameters that are obtained from this type of test.[4,5]

This paper presents some of the relevant results concerning an extensive mechanical characterization of a unidirectional graphite/polyimide (Gr/Pi). Tensile tests were conducted for a variety of off-axis angles with the objective of quantifying the influence of end constraints on the determination of the intralaminar shear modulus G_{12}.

Analysis

When a transversely isotropic tensile coupon is tested under off-axis loading conditions, the off-axis orientation effectively transforms the coupon into an anisotropic (monoclinic) specimen in the coordinate system coincident with the load axis. If the ends of the coupon are rigidly gripped and prevented from rotation (as dictated by a material's natural response) during applied pure axial displacement at the grips, a highly inhomogeneous state of deformation will be induced in the specimen. This has been referred to as 'the end-constraint effect.' It results in bending of the coupon in its own plane as illustrated in Fig. 1. The extent of such bending, and related inhomogeneity in the stress field, is a function of the specimen geometry (aspect ratio), material parameters and off-axis orientation (i.e., extent of shear-coupling present).

The first attempt to analyze the effect of end constraints in an off-axis tensile specimen was carried out by Pagano and Halpin.[3] The approach employed was that of a plane-stress elasticity formulation with idealized displacement boundary conditions at the grips. This approach facilitated an analytical, closed-form solution. Guided by experimental observation that the ends of a specimen tend to pull out from under the grips, the authors constrained only the center line of the specimen from rotation and thus were able to obtain closed form results. This would appear to be the most favorable fixed, rigid-grip formulation from the point of view of minimizing strain gradients induced by the gripping arrangement.

The basic results of the original paper by Pagano and Halpin have been essentially confirmed by a number of numerical and experimental studies.[4,6,7] However, with the exception of a limited analysis by Rizzo,[4] the main focus of the majority of studies was the effect of end constraints on the laminate Young's modulus E_{xx}. In this paper, the expression for the apparent intralaminar shear modulus G_{12}^{*}, in the presence of end constraints, is derived on the

M.-J. Pindera (SEM Member) is Assistant Professor and C.T. Herakovich (SEM Member) is Professor, Department of Engineering Science and Mechanics, Virginia Polytechnic Institute and State University, Blacksburg, VA 24061.

Original manuscript submitted: April 15, 1985. Final manuscript received: October 17, 1985.

basis of Pagano and Halpin's model and subsequently evaluated and compared with the corresponding expression for E^*_{xx}.

The relationship between the laminate stresses and strains at the midpoint of an off-axis tension coupon whose center line is prevented from rotation has been shown by Pagano and Halpin[3] to be of the following form:

$$\begin{Bmatrix} \epsilon_{xx} \\ \epsilon_{yy} \\ \gamma_{xy} \end{Bmatrix} = \begin{bmatrix} \overline{S}_{11} & \overline{S}_{12} & \overline{S}_{16} \\ \overline{S}_{12} & \overline{S}_{22} & \overline{S}_{26} \\ \overline{S}_{16} & \overline{S}_{26} & \overline{S}_{66} \end{bmatrix} \begin{Bmatrix} \sigma_{xx} \\ 0 \\ \tau_{xy} \end{Bmatrix} \tag{1}$$

with σ_{xx} and τ_{xy} given by

$$\begin{aligned} \sigma_{xx} &= C_2 \\ \tau_{xy} &= -C_0 h^2 \end{aligned} \tag{2}$$

where

$$\begin{aligned} C_0 &= \frac{6\overline{S}_{16}\epsilon_0}{6h^2(\overline{S}_{11}\overline{S}_{66} - \overline{S}_{16}^2) + \overline{S}_{11}^2 \ell^2} \\ C_2 &= \frac{C_0}{6\overline{S}_{16}}(6\overline{S}_{66}h^2 + \overline{S}_{11}\ell^2) \end{aligned} \tag{3}$$

ϵ_0 is the applied center-line strain which is constant, $\overline{S}_{ij}$ are the transformed compliances in the laminate coordinate system and h and ℓ are the half-width and length of the coupon, respectively.

Using eqs (2) and (3), τ_{xy} can be expressed in terms of σ_{xx} as follows:

$$\tau_{xy} = \beta\, \sigma_{xx} \tag{4}$$

where

$$\beta = -\frac{6\left(\frac{h}{\ell}\right)^2 \left(\frac{\overline{S}_{16}}{\overline{S}_{11}}\right)}{1 + 6\left(\frac{h}{\ell}\right)^2 \left(\frac{\overline{S}_{66}}{\overline{S}_{11}}\right)} \tag{5}$$

Furthermore, with the help of the expression for the total axial load P[3]:

$$P = t\int_{-h}^{+h} \sigma_{xx}\left(\frac{\ell}{2}, y\right)dy = 2th\left(C_2 - \frac{2}{3}\frac{\overline{S}_{16}}{\overline{S}_{11}}h^2 C_0\right) \tag{6}$$

the relation between average stress $\bar{\sigma}_{xx} = \frac{P}{2th}$ and midpoint stress σ_{xx} is obtained:

$$\sigma_{xx} = \frac{\bar{\sigma}_{xx}}{1 - \frac{2}{3}\eta} \tag{7}$$

where, following the notation of Halpin and Pagano, η is defined as:

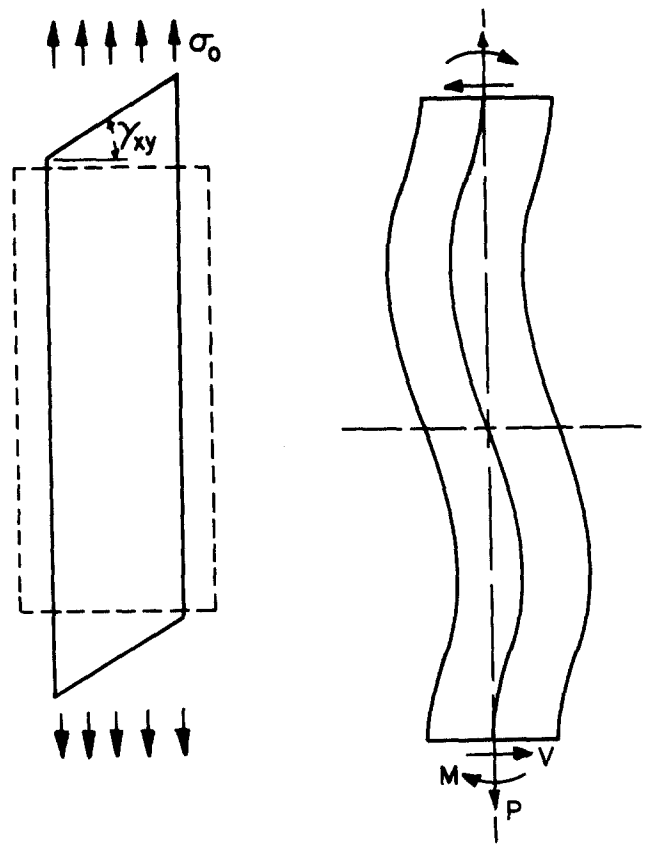

A) Uniform state of stress

B) Effect of clamped ends

Fig. 1—Influence of end constraints in the testing of anisotropic bodies, Ref. 3

$$\eta = \frac{6\left(\frac{h}{\ell}\right)^2\left(\frac{\bar{S}_{16}}{\bar{S}_{11}}\right)^2}{1 + 6\left(\frac{h}{\ell}\right)^2\left(\frac{\bar{S}_{66}}{\bar{S}_{11}}\right)} \tag{8}$$

Using the point transformation relations, the shear stress τ_{12} in the 1-2 coordinate system at the midpoint of the specimen is:

$$\tau_{12} = -\sigma_{xx}\sin\theta\cos\theta + \tau_{xy}(\cos^2\theta - \sin^2\theta) \tag{9}$$

where τ_{xy} is the shear stress in the laminate coordinate system induced by the end constraints in the presence of shear-coupling. Expressing τ_{xy} in the above equation in terms of σ_{xx} with the aid of eq (4), we obtain:

$$\tau_{12} = -\sigma_{xx}[\sin\theta\cos\theta - \beta(\cos^2\theta - \sin^2\theta)] \tag{10}$$

or, in terms of the average stress given by eq (7),

$$\tau_{12} = -\frac{\bar{\sigma}_{xx}}{\left(1 - \frac{2}{3}\eta\right)}[\sin\theta\cos\theta - \beta(\cos^2\theta - \sin^2\theta)] \tag{11}$$

However, in practice, it has been customary to ignore the shear stress contribution τ_{xy} induced by the end constraints as well as the resulting nonuniformity in the tensile stress across the width of the coupon with the result:

$$\tau_{12}^* = -\bar{\sigma}_{xx}\sin\theta\cos\theta \tag{12}$$

As will be subsequently illustrated, the shear stress in the material principal coordinates, τ_{12}, given by the correct transformation, eq (11), is smaller in magnitude for the considered composite system than the apparent shear stress τ_{12}^* given by eq (12) for a wide range of important test configurations. The difference between the correct and incorrect stress transformations in determining the shear response in the material principal coordinate system is graphically illustrated in Figs. 2(a) and 2(b), respectively.

The relation between the correct shear stress τ_{12} and the apparent shear stress τ_{12}^* is readily derived from eqs (11) and (12) in the following form:

$$\tau_{12} = \frac{\tau_{12}^*}{\left(1 - \frac{2}{3}\eta\right)}\left[1 - \frac{\beta(\cos^2\theta - \sin^2\theta)}{\sin\theta\cos\theta}\right] \tag{13}$$

Dividing the above relation by the shear strain γ_{12} and defining the apparent shear modulus $G_{12}^* = \frac{\tau_{12}^*}{\gamma_{12}}$, the following ratio, indicative of the error introduced in calculating the shear modulus, G_{12}, is obtained:

$$\frac{G_{12}}{G_{12}^*} = \frac{\tau_{12}}{\tau_{12}^*} = \frac{1 - \frac{\beta(\cos^2\theta - \sin^2\theta)}{\sin\theta\cos\theta}}{\left(1 - \frac{2}{3}\eta\right)} \tag{14}$$

The above derivation helps to bring forth the fact that the error is caused by the use of the incorrect transformation equation in calculating the resolved shear stress τ_{12}. If, on the other hand, all the stress components are properly considered in the course of resolving the stress and strain quantities given by eq (1) to the material principal coordinate system, the exact relation $G_{12} = \frac{\tau_{12}}{\gamma_{12}}$ is obtained. This rather obvious fact has been apparently overlooked by a number of researchers in the course of calculating the intralaminar shear modulus G_{12} on the basis of the off-axis tension test.

In a similar manner as that used to derive the expression for the apparent shear modulus G_{12}^*, the expression for

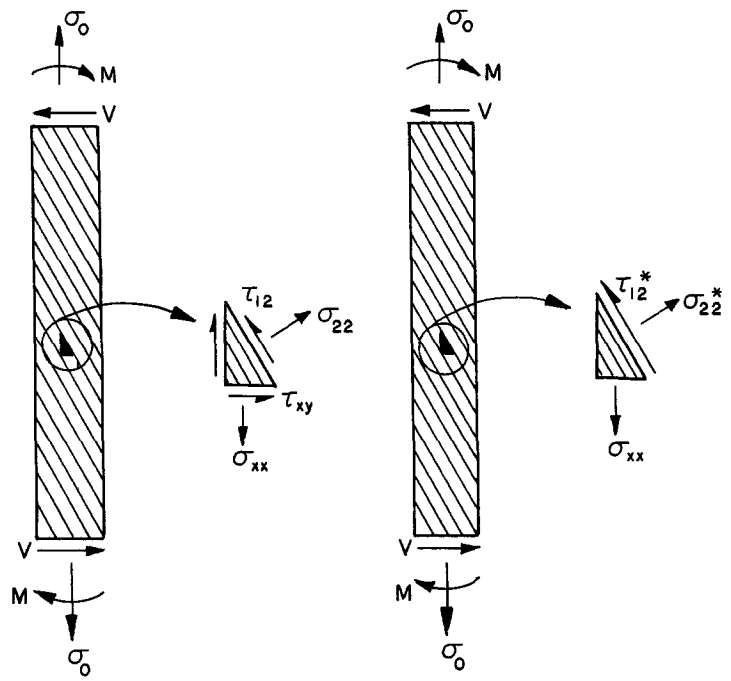

A) End Constraint Effect Included

B) End Constraint Effect Excluded

Fig. 2—Resolved shear stress in the material coordinate system with and without the influence of end constraints

the apparent laminate Young's modulus E^*_{xx} can be obtained as illustrated by Pagano and Halpin. Here, this expression is derived on the basis of the average laminate stress $\bar{\sigma}_{xx}$ as is commonly done in practice. Substituting the relation between τ_{xy} and σ_{xx} [eq (4)] and the relation between σ_{xx} and $\bar{\sigma}_{xx}$ [eq (7)] in the first of eqs (1) we obtain:

$$\frac{E_{xx}}{E^*_{xx}} = \frac{(1-\eta)}{(1-\frac{2}{3}\eta)} \tag{15}$$

For completeness, the result for the apparent laminate Poisson's ratio ν^*_{xy} is also presented:

$$\frac{\nu_{xy}}{\nu^*_{xy}} = \frac{1+(\frac{\bar{S}_{16}}{\bar{S}_{11}})\beta}{1+(\frac{\bar{S}_{26}}{\bar{S}_{12}})\beta} \tag{16}$$

At this point we note that the expression for the apparent shear modulus G^*_{12} given by eq (14) is not the same as that obtained from the familiar point-transformation relation (reproduced below with the apparent Young's modulus E^*_{xx} in place of E_{xx}) as employed by some authors.

$$\frac{1}{G^*_{12}} = \left[\frac{1}{E^*_{xx}} - \frac{\cos^4\theta}{E_{11}} - \frac{\sin^4\theta}{E_{22}}\right] \Big/ \cos^2\theta \sin^2\theta + \frac{2\nu_{12}}{E_{11}} \tag{17}$$

In effect, this particular method of evaluating the apparent shear modulus neglects certain stress components and results in somewhat different variations of G^*_{12} for different off-axis angles than those predicted by eq (14).

When comparing the error introduced in the determination of the shear modulus G_{12} and the Young's modulus E_{xx} with the end-constraint effect ignored, it is instructive to note that the general form of the equations for the respective apparent quantities is the same. Specifically, the second term in the numerator of eqs (14) and (15) (different in each case) represents the error due to the induced shear stress τ_{xy}, while the common denominator represents the error due to the nonuniformity of the applied axial stress across the width of the specimen. It is important to note that for $\theta = 45$ deg, the error due to τ_{xy} vanishes in calculating G_{12}.

Comparison of the error introduced in the determination of the shear modulus G_{12} and the laminate Young's modulus E_{xx} when the end-constraint effect is ignored is given in Figs. 3 and 4. Results are presented for three different aspect ratios (5, 10 and 20), values of G_{12} ranging from 5×10^5 psi to 9×10^5 psi, moduli $E_{11} = 19.81 \times 10^6$ psi, $E_{22} = 1.42 \times 10^6$ psi and major Poisson's ratio $\nu_{12} = 0.35$. An important conclusion from the above comparison is that the end-constraint phenomenon has a much more pronounced adverse effect on determination of G_{12} than on E_{xx}. The adverse effect is most pronounced for the low off-axis angles ($\theta < 30$ deg) and increases with decreasing specimen aspect ratio. Specifically, the error incurred in measuring E_{xx} for a 10-deg off-axis coupon with an aspect ratio of 10 is on the order of two to four percent. The corresponding error for G_{12} is on the order of 12-15 percent. As an added precaution we also note that the above values are conservative since they have been obtained on the basis of a model with somewhat idealized boundary conditions. Thus for a typical rigid-gripping arrangement the above errors could be actually higher; however, the relative magnitudes should not change significantly.

Reference 1 recommends the 10-deg off-axis specimen with an aspect ratio of at least 14 for determination of the intralaminar shear modulus G_{12}. For a 10-deg off-axis Gr/Pi specimen with an aspect ratio of 14, eq (12) predicts that the expected error range for G_{12} is at least six to eight percent. Even for very high aspect ratios such as 20, one can expect an error range of at least three to four percent for the Gr/Pi system considered.

Experimental Investigation

Test Fixture

The extent of the influence of end constraints discussed in the previous section depends on two different and perhaps interrelated phenomena: the rigid clamping of the specimen's ends and the prevention of rotation at the grips. Pagano and Halpin state in their study that the effect of clamping is the dominant factor. Wu and Thomas,[8] on the other hand, demonstrated experimentally that a rotating-type grip arrangement can noticeably reduce perturbations in the strain field. Their results were for 15-deg off-axis coupons with aspect ratios of 5, 4 and 2.5. A finite-element comparison between fixed-grip, rotating and nonrotating boundary conditions carried out by Rizzo[4] for several composite systems, aspect ratios and the 30-deg off-axis orientation, also indicated the desirability of using a rotating, fixed-grip arrangement for off-axis tests.

In view of the above observations a rotating-grip fixture was designed for the present study. The grip assembly is shown in Fig. 5. Although the primary objective of the fixture was to reduce the end-constraint effects, the design also eliminated alignment problems and resulted in excellent reproducibility of test data and gage section failures for most off-axis orientations.

Material System, Specimen Preparation and Instrumentation

The material employed for the experimental study was Celion 6000/PMR-15, a graphite/polyimide. Nine off-axis configurations (0, 5, 10, 15, 30, 45, 60, 75 and 90 deg) were cut from panels fabricated with prepreg at NASA-Langley according to in-house developed fabrication methods which utilized a drum-winding apparatus designed for this purpose.[9] The panels were rectangular plates, 26 in. by 50 in., the nominal thickness corresponding to a 12-ply layup, with the fiber direction parallel to the longer side. The ply thickness was a nominal 0.007 in. which resulted in a laminate thickness in the vicinity of 0.075 in. after cure, varying nominally by ± 0.005 in. This particular fabrication process employed in conjunction with the above prepreg yielded a nominal fiber-volume fraction of 60 percent. This was verified by cutting several pieces of material from various locations in the panels and leaching away the matrix material with a hot H_2SO_4 solution. The fiber-volume fractions recorded ranged from 59.77 to 62.51 percent. Furthermore, each panel was C-scanned after fabrication to determine the presence of defects. All panels were found defect-free upon examination of the C-scan photographs.

In order to have as homogeneous a set of specimens as possible, the glass transition temperature of each panel was determined. Some variation (100°F or so) was found in some samples and therefore each specimen was subjected to a post-cure cycle to achieve a glass-transition temperature of approximately 620°F for all coupons.

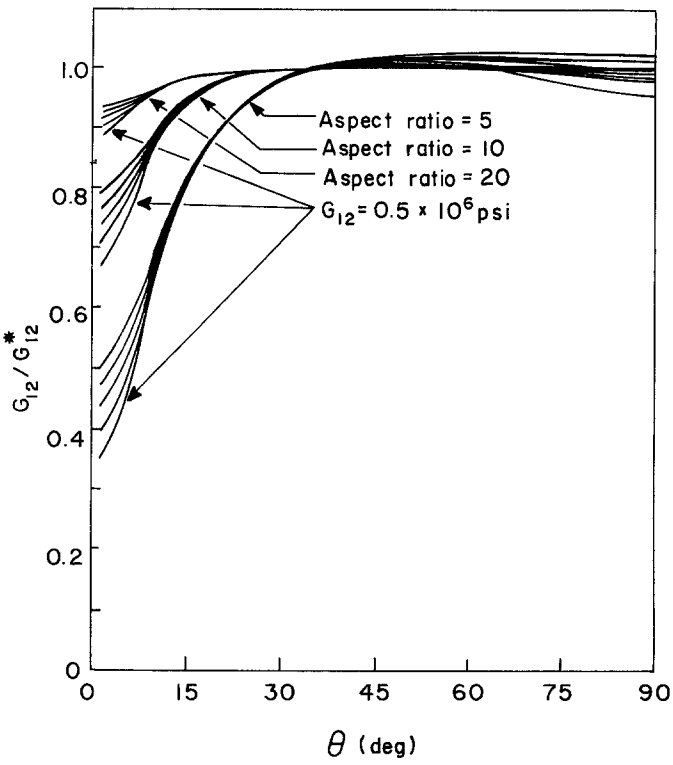

Fig. 3—Effect of end constraints on the determination of intralaminar shear modulus G_{12}

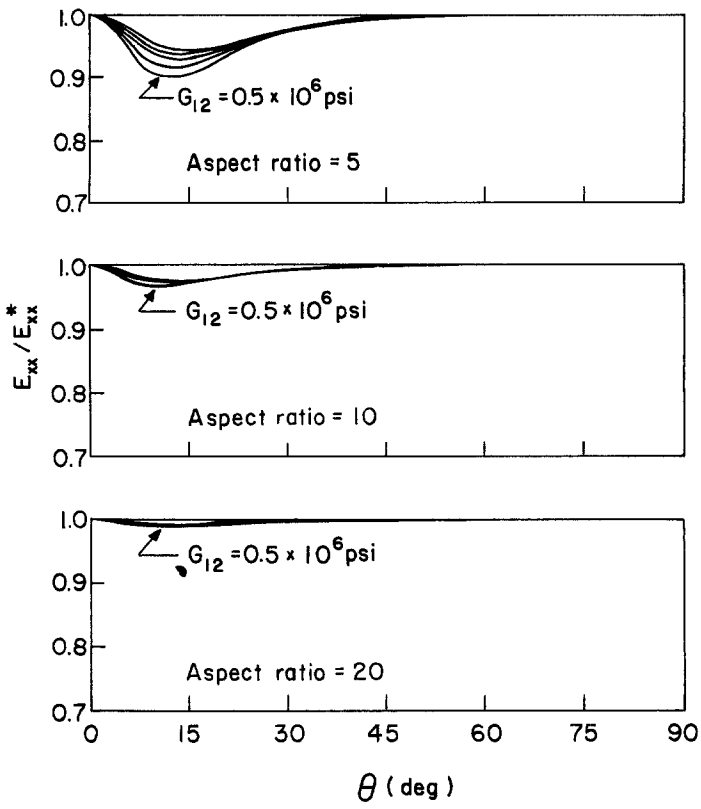

Fig. 4—Effect of end constraints on the determination of laminate Young's modulus E_{xx}

The specimens were nine inches long and a half inch wide with two inches allowed for gripping at either end. This yielded a test section with an aspect ratio of ten. Each specimen was strain gaged with a single Micro-Measurements 45-deg rosette WK-06-060WR-350 bonded at the midpoint of the coupon and a uniaxial gage WK-06-062AP-350 mounted back-to-back with the rosette. The alignment of each strain gage was checked under a microscope and misalignment angles with respect to the coupon's longitudinal axis were recorded for data-reduction purposes. Generally, the misalignment angle was found to be small: less than 1.0 deg in the majority of cases. A photograph showing the dimensions of the 45-deg rosette and uniaxial gage with respect to the coupon's width is given in Fig. 6.

Test Procedure, Data Acquisition and Reduction

All tests were carried out with a displacement-rate controlled Instron tensile machine at a fixed crosshead speed that yielded an average strain rate of one percent per minute. The data-acquisition system consisted of Vishay 2120 wheatstone bridges, an HP3495A scanner with an a–d converter and a Tektronix 4051 minicomputer which automatically recorded the output data on tape. Load and strain were sampled at approximately 1.6 pt/sec.

The reduction of experimental data was carried out with the help of a computer program that included the following features: correction for the small strain-gage misalignment, bending and gage transverse sensitivity effects and calculation of stresses based on a cross-sectional area at the midpoint of the specimen. The above were accomplished in the following fashion. First, the strain components in the coordinate system of the rosette were transformed (after evaluating the shear component γ_{xy} through the appropriate transformation equations of a 45-deg three-arm rosette) to the coordinate system of the uniaxial gage located on the reverse side of the specimen. In general, because of small misalignment, the longitudinal axes of these gages were not coincident with each other and with the coupon's axis, although this misalignment was typically less than 1 deg and often less than ½ deg as mentioned previously. Subsequently, the transverse-sensitivity effects were eliminated using the well-known relations.[10] The amount of bending was determined by comparing the strain outputs of the longitudinal gages and subsequently used to eliminate bending effects in all the arms of the rosette. These were found to be quite small due to self-aligning features of the particular test fixture employed. The resulting corrected strains were then transformed to the material-principal-coordinate system by taking into account the orientation of the coordinate system in which the rosette strains were corrected with the actual orientation of the fibers. Transformation of the applied stress to the material-principal-coordinate axes completed the determination of various response characteristics along the material principal directions.

Experimental Results

The results for the apparent shear stress–strain response along the material principal directions for the off-axis orientations employed in the present study are presented in Fig. 7. Representative curves of several monotonic tests for each orientation are given. It is important to mention that the scatter in the initial shear response for the individual off-axis orientations was quite small.

The experimentally determined apparent shear moduli of the different configurations tested are presented in Fig. 8. These moduli approach an asymptotic value of approximately 0.725×10^6 psi for off-axis angles greater than 45 deg. Also presented are the predictions for the apparent shear modulus in the presence of end-constraint effects obtained from eq (14) and the experimental shear moduli corrected for this effect on the basis of the aforementioned equation. The following experimentally determined material parameters have been employed to obtain predictions of eq (14): $E_{11} = 19.81 \times 10^6$ psi, $E_{22} = 1.42 \times 10^6$ psi, $\nu_{12} = 0.35$ and the asymptotic value of G_{12} given above. It is important to note the rather severe effect of end constraints in the region θ deg ≤ 30 deg. This effect appears to be greater for this particular gripping arrangement than that predicted on the basis of the

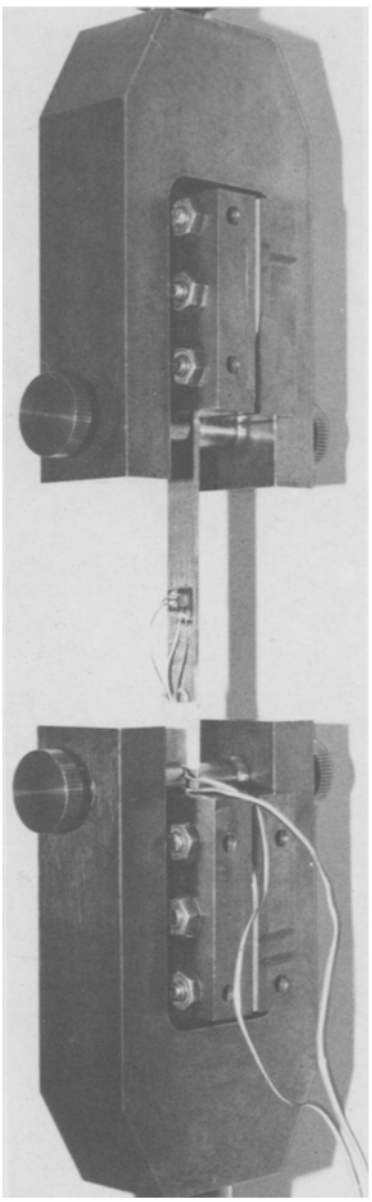

Fig. 5—Rotating end-grip test-fixture assembly

approximate model of Pagano and Halpin. However, it is also evident that the use of the approximate model in correcting for the effect of end constraints significantly reduces the error in calculating the shear modulus G_{12}.

Table 1 summarizes the above experimental and analytical results.

For completeness, the experimental results for the laminate Young's modulus E_{xx} and the Poisson's ratio

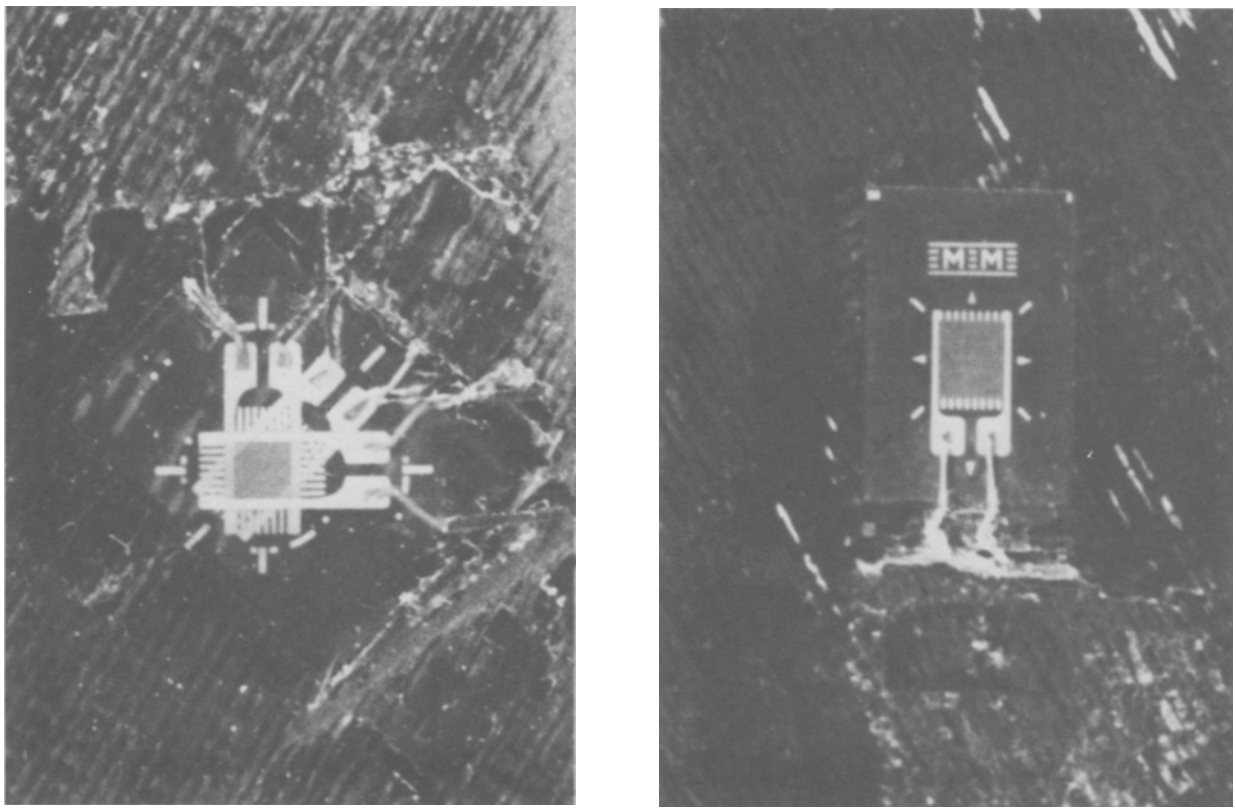

Fig. 6—Specimen-mounted strain gages

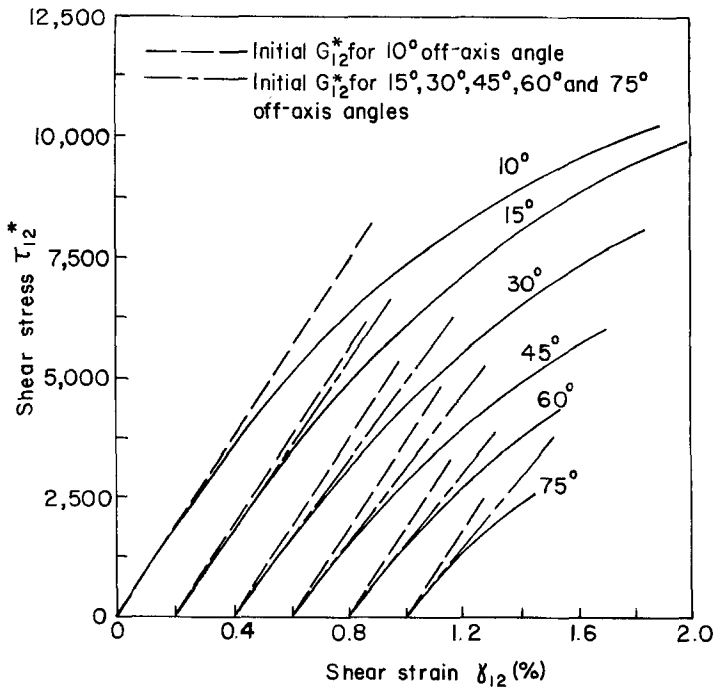

Fig. 7—Apparent shear stress-strain response in the material coordinate system for different off-axis configurations

ν_{xy}, summarized in Table 2, are compared with theoretical predictions of the transversely isotropic transformation equations in Figs. 9 and 10. The corresponding apparent quantities given by eqs (15) and (16) which have been calculated using the above-mentioned asymptotic value of the shear modulus G_{12} are also included for comparison. It can be concluded from the presented data that the composite material employed in the present study can be modeled very well as a transversely isotropic system. Furthermore, while the deviation in experimental data from the predicted response can be explained on the basis of the end-constraint effect with the aid of the Pagano-Halpin model in the case of the Poisson's response, these deviations are somewhat larger in the high shear-coupling region (10 deg $\leq \theta \leq$ 20 deg) for the laminate Young's modulus E_{xx}. However, it is important to note that the trends observed in the experimental data are essentially the same as those predicted by the idealized model. That is, the deviation in E_{xx} is greatest for the 10-deg off-axis specimen followed by the 15-deg specimen and finally followed by the 5-deg specimen as is evident in Fig. 9.

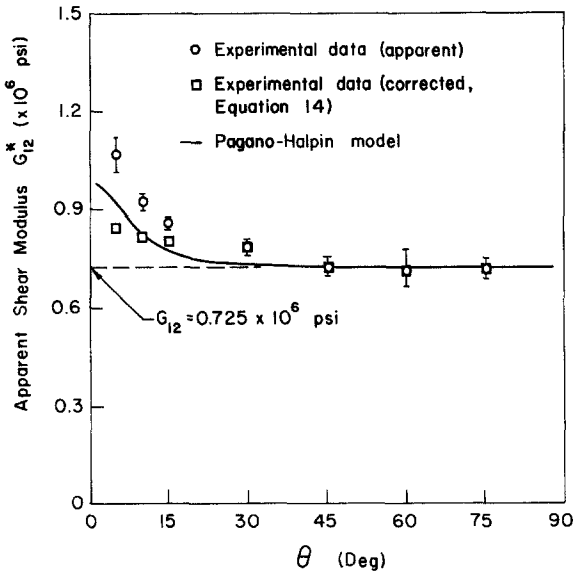

Fig. 8—Measured intralaminar shear modulus G^*_{12} of different off-axis configurations

Discussion

The experimental and analytical evidence presented here points to the important influence of the end-constraint phenomenon on the determination of the intralaminar shear modulus G_{12} of highly anisotropic unidirectional composites. Specifically, the error introduced by the end constraints in the presence of shear-coupling affects accurate determination of G_{12} more adversely than it affects the laminate Young's modulus E_{xx}. The error in G_{12} can be significant in the low off-axis region for aspect ratios which are normally deemed high. For the particular Gr/Pi system employed in the present study, 10-deg off-axis specimens with an aspect ratio of 10 yielded results for the Young's modulus E_{xx} and the intralaminar shear modulus G_{12} which were 14 percent and 27 percent higher, respectively, than the corresponding true values of an ideal transversely isotropic system. These variations are higher than those predicted by the idealized model developed by Pagano and Halpin despite the fact that a special test fixture designed to reduce end-constraint effects has been employed in the present study. In view of the fact that the above variations are more than two times larger than those predicted by the idealized model mentioned above, it would appear that specimens with very high aspect ratios are required to eliminate the adverse effect of end constraints for accurate determination of the intralaminar shear modulus G_{12} for this particular material. Consequently, for certain classes of highly anisotropic unidirectional composites the 10-deg off-axis coupon is not a practical test configuration.

On the other hand, both the experimental and analytical data presented here indicate that, even for highly anisotropic composites such as Gr/Pi, the effect of end constraints on the determination of G_{12} becomes negligible for off-axis angles equal to or greater than 45 deg. Furthermore, at θ = 45 deg, the influence of the laminate shear stress τ_{xy} vanishes. As the 45-deg configuration still yields sufficiently large shear stress and strain values for accurate determination of the initial shear response, it is recommended for such characterization in the case of highly anisotropic unidirectional composites. Figure 11 presents the variation of G_{12}/G^*_{12} for different aspect ratios of the considered Gr/Pi system when θ = 45 deg as an illus-

TABLE 1—EXPERIMENTAL, APPARENT AND CORRECTED SHEAR MODULI OF DIFFERENT OFF-AXIS CONFIGURATIONS TESTED

θ Off-Axis Angle (deg)	$\frac{G_{12}}{G^*_{12}}$ Pagano-Halpin eq (14)	G^*_{12} Experimental, Apparent	G_{12} Experimental, Corrected*	Percent error Experimental, Uncorrected† (percent)	Percent Error Experimental, Corrected† (percent)
5	0.7919	10.69 x 10^5 psi	8.46 x 10^5 psi	47.4	16.7
10	0.8812	9.25	8.15	27.6	12.4
15	0.9395	8.58	8.06	18.3	11.2
30	0.9942	7.86	7.81	8.4	7.7
45	1.0038	7.23	7.25	−0.3	0.0
60	1.0046	7.10	7.13	−2.0	−1.6
75	1.0026	7.13	7.15	−1.6	−1.4

Corrections based on eq (14), second column of Table 1
†Based on the asymptotic value G_{12} = 0.725 x 10^6 psi, taken as the 'true' value

tration in choosing an optimal specimen configuration from the points of view of both accuracy and practicality. However, as the 10-deg off-axis configuration yields significantly higher shear stresses at failure, it is still the preferred specimen for estimating the shear strength of unidirectional composites. At this orientation, the shear stress in the principal-material-coordinate system is the major contributor to fracture. It is worthwhile to add, however, that the resulting value of τ_{12} at failure will be in error unless all stresses are properly resolved. Equation (14) indicates the extent of error that results when end-constraint effects are neglected.

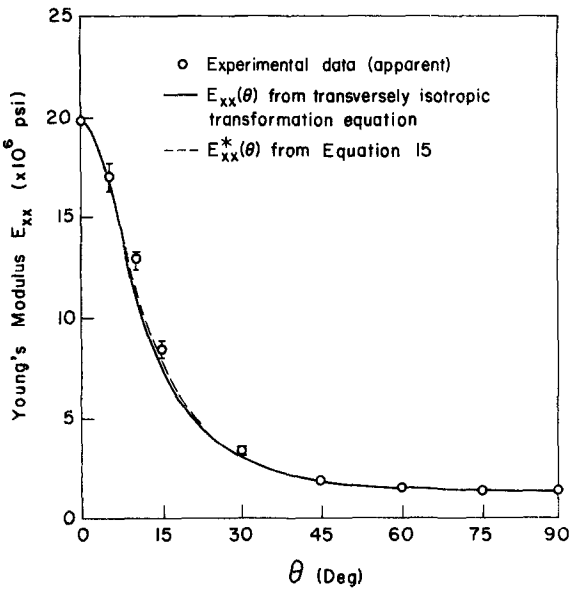

Fig. 9—Measured laminate Young's modulus E^*_{xx} as a function of the off-axis angle

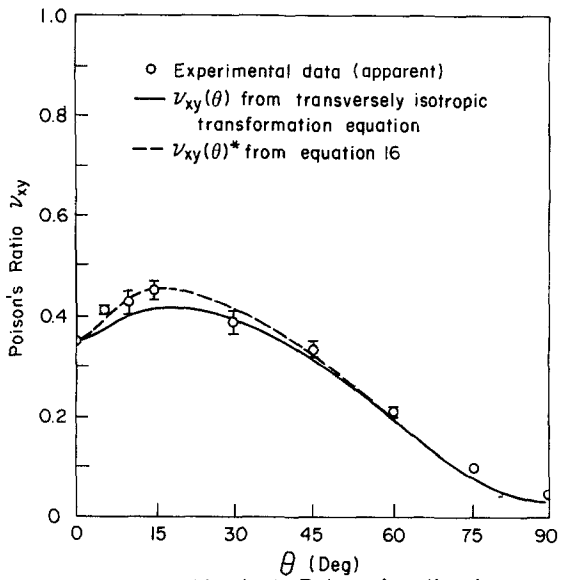

Fig. 10—Measured laminate Poisson's ratio ν^*_{xy} as a function of the off-axis angle

Conclusions

The following important conclusions based on the experimental and analytical results of the present study are briefly summarized below.

(1) In the course of transforming laminate stresses to a material-principal-coordinate system, all the stress components—including those induced by end constraints in the presence of shear-coupling—should be included.

(2) The error introduced by end constraints in an off-axis tension test has a significantly larger adverse effect on accurate determination of the intralaminar modulus G_{12} than the laminate Young's modulus E_{xx} in the region $\theta \leq 30$ deg.

(3) For highly anisotropic composites, very long and slender 10-deg off-axis specimens are required to reduce the error in G_{12} caused by the end-constraint effect to an acceptable level.

(4) The 45-deg off-axis coupon is an excellent specimen for accurate determination of the intralaminar shear modulus G_{12}.

TABLE 2—AVERAGE VALUES OF THE MEASURED ELASTIC MODULI FOR DIFFERENT OFF-AXIS ORIENTATIONS

θ Off-Axis Angle (deg)	E^*_{xx} Laminate Young's Modulus (Msi)	ν^*_{xy} Laminate Poisson's Ratio
0	19.81	0.350
5	17.16	0.414
10	12.89	0.430
15	8.54	0.450
30	3.36	0.391
45	1.95	0.338
60	1.53	0.218
75	1.45	0.101
90	1.42	0.047

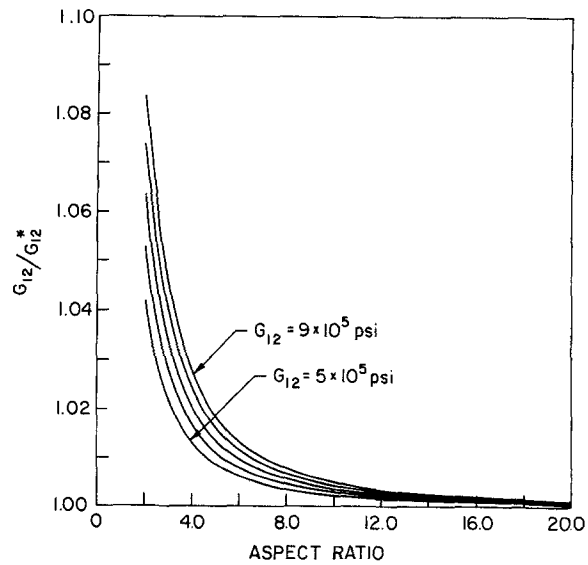

Fig. 11—Effect of end constraints on the determination of intralaminar shear modulus G_{12} for θ = 45 deg

(5) Practical aspect ratios can be employed for calculating G_{12} with the 45-deg off-axis coupon.

Acknowledgment

This work was supported by the NASA-Virginia Tech Composites Program, NASA CA NCC1-15. The authors gratefully acknowledge this support.

References

1. Chamis, C.C. and Sinclair, J.H., "Ten-Degree Off-Axis Test for Shear Properties in Fiber Composites," EXPERIMENTAL MECHANICS, **17** (9), 339 (Sept. 1977).
2. Chamis, C.C., "Failure Criteria for Filamentary Composites," STP 460, Composite Materials: Testing and Design, ASTM, New Orleans, 336 (1972).
3. Pagano, N.J. and Halpin, J.C., "Influence of End Constraints in the Testing of Anisotropic Bodies," J. Comp. Mat., **2** (1), 18 (Jan. 1968).
4. Rizzo, R.R., "More on the Influence of End Constraints on Off-Axis Tensile Tests," J. Comp. Mat., **3**, 202 (April 1969).
5. Pindera, M.J. and Herakovich, C.T., "An Endochronic Theory for Transversely Isotropic Fibrous Composites," VPI-E-81-27, Virginia Polytechnic Instit. and State Univ., Blacksburg, VA (Oct. 1981).
6. Richards, G.L., Airhart, T.P. and Ashton, J.E., "Off-Axis Tensile Coupon Testing," J. Comp. Mat., **3**, 586 (July 1969).
7. Nemeth, M.P., Herakovich, C.T. and Post, D., "On the Off-Axis Tension Test for Unidirectional Composites," Comp. Tech. Rev., **5** (2), 61 (Summer 1983).
8. Wu, E. and Thomas, R., "Note on the Off-Axis Test for a Composite," J. Comp. Mat., **2**, 523 (1968).
9. Davis, J.G., Jr., ed., "Composites for Advanced Space Transportation Systems - (CASTS)," NASA TM 80038 (1979).
10. "Errors Due to Transverse Sensitivity," M-M Tech Note TN-137: Transverse Sensitivity Errors, Measurements Group, Inc., Raleigh, NC.

Analysis of Residual Stresses in Cylindrically Anisotropic Materials

Paper by G.Z. Voyiadjis, P.D. Kiousis and C.S. Hartley appears in the June 1985 issue of EXPERIMENTAL MECHANICS, pages 145-147

Discussion

by Charles W. Bert

The discusser found this paper to be of considerable interest, especially since he was the co-author of a paper with a similar objective published in the same journal 19 years earlier.[1] The 1966 paper also provided suggestions on means of measuring the cylindrically anisotropic-elastic properties and curves of the percentage error in the radial and circumferential stresses. In contrast, the 1985 paper includes not only the case of material removed from the inside surface (treated in the 1966 paper) but also that of material removed from the outside surface and the case of residual shear stresses due to torsion.

One other point is that in spite of the more general title of the 1985 paper, it considers the same class of material as the 1966 paper: cylindrically orthotropic. More complicated cases of cylindrical anisotropy, such as the cylindrically monoclinic case investigated in Ref. 2, involve more elastic constants than those considered in either the 1966 or 1985 papers.

References

1. Olson, W.A. and Bert, C.W., "Analysis of Residual Stresses in Bars and Tubes of Cylindrically Orthotropic Materials," EXPERIMENTAL MECHANICS, **6** (9), 451-457 (1966).
2. Vanderpool, M.E. and Bert, C.W., "Vibration of a Materially Monoclinic, Thick-wall Circular Cylindrical Shell," AIAA J., **19** (5), 634-641 (1981).

Charles W. Bert (SEM Fellow) is Benjamin L. Perkinson Professor of Engineering, School of Aerospace, Mechanical and Nuclear Engineering, The University of Oklahoma, Norman, OK 73019.

Author's Closure

The authors agree with Professor Bert that the term "cylindrically orthotropic" more accurately describes the elastic symmetry considered in this paper. Although "cylindrical anisotropy" implies a wider range of symmetries than are treated in the analysis, it is not an incorrect designation since cylindrical orthotropy is a special case of cylindrical anisotropy. We are particularly grateful to Professor Bert for bringing his previous work to our attention. Our work not only confirms his earlier results but also extends the analysis to include the important cases of material removal from the outer surface and the presence of residual shear stresses in the tube wall. The equations developed in our work permit a parametric study of the effect of the degree of orthotropy on the calculated stresses, as was presented in the paper by Olson and Bert for the case that they studied.